Nuclear Instruments and Methods in Physics Research A 652 (2011) 288–291

Contents lists available at ScienceDirect

Nuclear Instruments and Methods in Physics Research A

journal homepage: www.elsevier.com/locate/nima

The role of hole mobility in scintillator proportionality

Qi Li [a,*], Joel Q. Grim [a], R.T. Williams [a], G.A. Bizarri [b], W.W. Moses [b]

[a] Department of Physics, Wake Forest University, Winston-Salem, NC 27109, USA
[b] Lawrence Berkeley National Laboratory, Berkeley, CA 94720, USA

ARTICLE INFO

Available online 1 August 2010

Keywords:
Nonproportionality
Carrier diffusion
Mobility
CsI:Tl
HPGe
Semiconductor scintillator

ABSTRACT

Time-dependent radial diffusion and drift are modeled in the high carrier concentration gradient characteristic of electron tracks in scintillators and other radiation detector materials. As expected, the lower mobility carrier (typically the hole) controls the ambipolar diffusion. Carrier separation when electron and hole mobilities are unequal produces a built-in radial electric field near the track analogous to an *n-intrinsic* semiconductor junction. The diffusion is shown to have significant effects on both the low dE/dx and high dE/dx ends of electron light-yield curves and their respective contributions to nonproportionality. In CsI:Tl, it is shown that electron confinement toward the end of the track accentuates high-order quenching such as Auger recombination or dipole–dipole transfer, while in HPGe extremely rapid (<1 fs) dilution of carrier concentration by radial diffusion renders Auger quenching negligible. Separation of geminate carriers is accentuated in the beginning of the track if electron and hole mobilities are widely unequal as in CsI:Tl, leading to bimolecular recombination of trapped carriers by slower thermal hopping routes as the favored channel at low dE/dx.

1. Introduction

It is generally assumed that the root cause of nonproportionality in scintillators is nonradiative electron–hole recombination (quenching) that depends nonlinearly on the ionization density, coupled with the variability of local ionization density from beginning to end of an electron track. In order to relate dE/dx to a volume density of excitations that enter the 2nd and 3rd order nonradiative decay rates associated with dipole–dipole transfer and Auger recombination, it is necessary to know the (time-dependent) radius of the distribution of excitations. For example if one models the linear deposition dE/dx locally as distributed in a cylindrical track of radius r_t, then the excitation density at any location along the track is proportional to $(dE/dx)/r_t^2$ at that point. Clearly, the nonlinear quenching processes are very sensitive to $r_t(t)$, being 4th order in r_t for dipole–dipole and 6th order for Auger quenching.

We can associate three characteristic time ranges of changing $r_t(t)$ with different physical processes of radial diffusion: (1) ballistic transport of carriers created with kinetic energy in excess of kT, lasting for a thermalization time of femtosecond to picosecond, during which the carriers diffuse a thermalization length l_t [1]; (2) diffusion of carriers with band mobilities in thermal equilibrium, commencing at the end of ballistic transport and continuing until the carrier is recombined with a partner or reduced to slow thermal hopping transport after becoming trapped; and (3) thermal hopping/detrapping on a time scale of nanoseconds to microseconds in room temperature scintillators [2]. Process (1) of ballistic transport is often folded into the definition of an initial track radius. Vasil'ev has estimated a thermalization length $l_t=3$ nm as typical for scintillator materials [1]. It is the process (2) of band diffusion in thermal equilibrium that is the topic of this paper, having importance in $\sim$20 ps down to $\sim$1 fs depending on mobilities. If diffusion/drift produces a significant dilution of concentration on this time scale, it can exert a strong influence on the outcome of Auger and dipole–dipole quenching, flattening the roll-off of light yield at high dE/dx. If it introduces spatial separation of electrons and holes, it can influence the path of radiative recombination kinetics and trap-mediated quenching. The diffusive separation of electrons and holes due to unequal mobilities will be shown to be favored at low dE/dx, especially when holes are immobile (self-trapped). In this way diffusive band transport of electrons relative to holes on the picosecond time scale can explain why the depression of light yield at low dE/dx is a feature peculiar to halide scintillators and is especially strongly expressed in NaI:Tl, CsI:Tl, and CsI:Na where holes are known to be strongly self-trapped. To illustrate these effects, we will compare diffusion simulations in a scintillator with nearly zero hole mobility on the relevant time scale (CsI:Tl) and in high-purity germanium (HPGe) semiconductor detector material having very high hole and electron mobilities.

* Corresponding author.
E-mail address: liq9@wfu.edu (Q. Li).

0168-9002/$ - see front matter © 2010 Elsevier B.V. All rights reserved.
doi:10.1016/j.nima.2010.07.074

2. Modeling method

Time-step finite-element analysis was used to solve for the diffusion and drift currents, electric field, and local carrier concentration in cylindrical symmetry around the track of a charged particle. The equations used are

$$\vec{J}_e(\vec{r},t) = -D_e \nabla n_e(\vec{r},t) - \mu_e n_e(\vec{r},t)\vec{E}(\vec{r},t) \quad (1)$$

$$\frac{\partial n_e(\vec{r},t)}{\partial t} = -\nabla \cdot \vec{J}_e(\vec{r},t) \quad (2)$$

for electrons and an equivalent set of equations for holes, where the variables and constants have their usual meanings. Gauss's law:

$$\nabla \cdot \vec{E}(\vec{r},t) = \frac{\rho}{\varepsilon \varepsilon_0} \quad (3)$$

serves to evaluate electric field for insertion back into the diffusion/drift equation. The Einstein relation $D=\mu k_B T/e$ gives the diffusion coefficients for electrons and holes in terms of their mobilities μ_e and μ_h. The static dielectric constant ε of the material is used in Gauss's law.

The finite-element evaluation is applied to cylindrical shells around a starting distribution, which is taken to be a Gaussian radial profile initially identical for electrons and holes. The electron and hole number in each cylindrical shell is updated in each time step according to the diffusion and drift currents across the cell boundaries. When it is desired to evaluate Auger quenching, a 3rd-order loss corresponding to Eq. (4) is included in the right side of Eq. (2) for evaluation in each cell and time step.

$$\frac{\partial n(\vec{r},t)}{\partial t} = -\gamma n^3(\vec{r},t) \quad (4)$$

Following the approximate treatment of Ref. [3], the concentration n in intrinsic material is taken to refer to free electrons or free holes equivalently.

Driven by the huge concentration gradient posed by up to 3×10^{20} electrons/cm^3 confined initially within a radius of 3 nm, the electrons diffuse outward, opposed by drift back toward the collection of immobile (on this time scale) self-trapped holes in the example of CsI or virtually un-opposed in Ge. We incorporated in the model a test to determine on average whether a geminate e–h pair gets ripped apart by the difference in electron and hole diffusion currents at a given radial position and time. By evaluating the currents at the boundaries of each cell, the model can determine the integrated current flowing through a given cell up to a time t. Dividing that current by the electron concentration within the cell gives the average total displacement of electrons comprising the current at that place and time. Since the holes are immobile in the alkali halides on this time scale, electron displacement specifies the average displacement of an electron from its geminate hole partner *attributable to the mismatch of mobility-related electron and hole diffusion currents*. To the extent that this displacement, occurring in the average time t_{Tl} for trapping a carrier on an activator, exceeds the average spacing of Tl^+ activator ions in the crystal, then the electron will on average be trapped on a *different* Tl^+ (forming Tl^0) than will the hole (forming Tl^{++} on a different site). Subsequent recombination via this channel will be of 2nd order, which will proceed by a slower route of carrier de-trapping and re-trapping and can be subject to deep trapping or extra nonradiative recombination channels. On the other hand, if the electron and hole are not ripped apart in the contest of diffusion and drift, they are more likely to be captured on the *same* Tl^+ in their vicinity and to undergo prompt monomolecular radiative decay. A related test applies in the more general case where both carriers are mobile.

3. Results and discussion

At room temperature, the average self-trapped hole (STH) jump rate in CsI is $1.7\times10^9\ s^{-1}$ [2]. Thus, for purposes of the simulations of band diffusion in $\lesssim$20 ps presented here, the hole mobility in CsI is effectively $\mu_h=0$. The electron mobility in pure CsI has been measured as $\mu_e=8$ cm^2/Vs at room temperature [4], and the static dielectric constant $\varepsilon=5.65$. We specify thallium doping level (0.3%) because of its role in the test for geminate-to-independent branching. HPGe has $\mu_h=42{,}000$ cm^2/Vs and $\mu_e=36{,}000$ cm^2/Vs at its 77 K operating temperature [5] and $\varepsilon=16$. The measured Auger rate constant in Ge is $\gamma=1.1\times10^{-31}$ cm^6/s [3]. A measured Auger rate constant is not available for CsI, so we assigned the Ge Auger rate constant to CsI for the sake of comparing purely the diffusion effects on Auger decay, all else being kept the same. Vasil'ev has estimated that the maximum electron–hole pair density produced on-axis near the track end of an energetic electron is about 2×10^{20} cm^{-3} in NaI [1]. Therefore we have modeled hole and electron diffusion at initial on-axis concentrations of 2.5×10^{18} up to 2.5×10^{20} cm^{-3} for CsI:0.3%Tl and for HPGe (77 K). Both cases assume a starting Gaussian radius of 3 nm. For immobile holes as in CsI, the diffusion and drift currents come to a balance at a steady-state time t_{ss} ranging from 9 to 0.4 ps for on-axis carrier densities of 2.5×10^{18} and 2.5×10^{20} cm^{-3}, respectively. Such a steady state distribution is analogous to a p–n junction or more specifically a cylindrical *n-intrinsic* junction with depletion zone and built-in electric field, where the role of ionized donors is played by the immobile holes. Just as electrons thermally released from the donors diffuse beyond the sharply defined boundary of the doped region, setting up charge separation and a built-in electric field, so do conduction electrons excited from the valence band diffuse relative to the sharply confined core of self-trapped holes [1]. By contrast, the e^{-1} radial profile of both carriers in HPGe has already expanded within 1 fs by a factor 6.5 times the starting radius r_{t_0}, rendering the Auger decay rate, proportional to $(r_t)^{-6}$, negligible for $t>1$ fs.

Fig. 1 compares the e^{-1} radius of electron distribution versus on-axis initial density n_0 for CsI and HPGe, both having started from the same 3 nm Gaussian distribution. The CsI radius contour is shown at 1000 fs, whereas the Ge contour has already expanded to a much larger radius in 1 fs, and will go out of the range plotted in the next femtosecond. The extreme contrast in the diffusive track expansion rates for these two materials is the first lesson of Fig. 1. As we have pointed out that the 2nd and 3rd order quenching processes are 4th and 6th order in the instantaneous

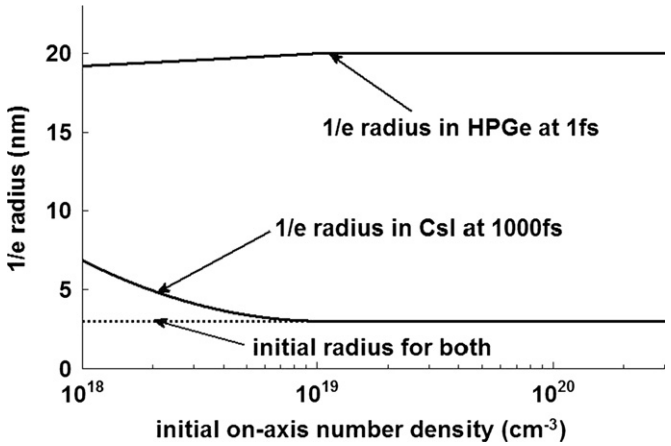

Fig. 1. Comparison of the post-diffusion e^{-1} radius contours of electron population in HPGe after 1 fs and in CsI after 1000 fs versus initial on-axis density of electrons and holes.